

RESEARCH ARTICLE

Open Access



Gene expression analysis of skin grafts and cultured keratinocytes using synthetic RNA normalization reveals insights into differentiation and growth control

Shintaro Katayama¹, Tiina Skoog¹, Eeva-Mari Jouhilahti¹, H. Annika Siitonen^{2,3}, Kristo Nuutila⁴, Mari H Tervaniemi^{2,3}, Jyrki Vuola⁵, Anna Johnsson⁶, Peter Lönnerberg⁶, Sten Linnarsson⁶, Outi Elomaa^{2,3}, Esko Kankuri^{4*} and Juha Kere^{1,3,7*}

Abstract

Background: Keratinocytes (KCs) are the most frequent cells in the epidermis, and they are often isolated and cultured *in vitro* to study the molecular biology of the skin. Cultured primary cells and various immortalized cells have been frequently used as skin models but their comparability to intact skin has been questioned. Moreover, when analyzing KC transcriptomes, fluctuation of polyA⁺ RNA content during the KCs' lifecycle has been omitted.

Results: We performed STRT RNA sequencing on 10 ng samples of total RNA from three different sample types: i) epidermal tissue (split-thickness skin grafts), ii) cultured primary KCs, and iii) HaCaT cell line. We observed significant variation in cellular polyA⁺ RNA content between tissue and cell culture samples of KCs. The use of synthetic RNAs and SAMstrt in normalization enabled comparison of gene expression levels in the highly heterogenous samples and facilitated discovery of differences between the tissue samples and cultured cells. The transcriptome analysis sensitively revealed genes involved in KC differentiation in skin grafts and cell cycle regulation related genes in cultured KCs and emphasized the fluctuation of transcription factors and non-coding RNAs associated to sample types.

Conclusions: The epidermal keratinocytes derived from tissue and cell culture samples showed highly different polyA⁺ RNA contents. The use of SAMstrt and synthetic RNA based normalization allowed the comparison between tissue and cell culture samples and thus proved to be valuable tools for RNA-seq analysis with translational approach. Transcriptomics revealed clear difference both between tissue and cell culture samples and between primary KCs and immortalized HaCaT cells.

Background

Skin is a multi-layered tissue that is composed of continuously renewing epidermis – with keratinocytes (KCs) as a predominant cell type – and underlying dermis populated mostly by fibroblasts. The life span of epidermal keratinocytes is controlled by two alternative pathways: differentiation as their normal function or activation as an altered function in wound healing or skin diseases [1]. Epidermal KCs residing in the basal layer of the epidermis

differentiate through multiple layers and finally shed as cornified dead cells from the skin surface [2, 3].

The relatively noninvasive sampling together with the methods that allow culturing of pure KCs have greatly facilitated research on skin and KCs. In cell culture, KCs are uncoupled from their tissue environment that naturally provides a network of homeostatic control signals; they are induced to either retain an active proliferative state or to differentiate. However, the prolonged KC culturing leads to the induction of cellular senescence [4] and therefore not only primary KCs but also immortalized KC lines, such as HaCaT (a spontaneously immortalized cell line) [5], have been widely studied to understand various normal and altered functions of the skin. HaCaT cells represent a highly popular model system since despite some

* Correspondence: esko.kankuri@helsinki.fi; juha.kere@ki.se

⁴Department of Pharmacology, Faculty of Medicine, University of Helsinki, Helsinki, Finland

¹Department of Biosciences and Nutrition, Karolinska Institute and Center for Innovative Medicine, Huddinge, Sweden

Full list of author information is available at the end of the article

UV-inducible mutations in *TP53* alleles [6, 7] they are non-tumorigenic and have retained their capacity to differentiate [5, 7, 8]. The comparability of each of the models to intact skin has often been questioned. In the current study, we address the question of how representative models cultured KCs and HaCaTs are for studying human epidermis.

Genome-wide expression profiling is an useful approach to screen key genes with respect to different cellular statuses and to further model the regulatory networks [9]. Microarray technology provides a traditional profiling method to measure thousands of known genes simultaneously, but it has recently been replaced by RNA-seq technology that has proven to give more detailed insights into transcriptome. Both technologies have been previously applied to study the gene expression in skin [10–12]. However, an important fact has been largely omitted: when KCs undergo their complex lifecycle, they change not only cell size and cell cycle kinetics, but also the actively transcribed RNA content, with the largest RNA content in fresh, actively growing cultured KCs [13]. In microarray, RNA-seq and even qRT-PCR, the same amount of total RNA is loaded for each sample, although yields of the polyA+ RNAs purified from total RNAs may differ. Moreover, normalization for the differential expression test expects equivalent expression levels for several co-expressed genes [14]. Therefore, the genome-wide expression profiling in the previous studies might have underestimated the complexity of the KC transcriptome during their lifecycle.

In this study, we revisit the skin and KC transcriptome with respect to fluctuation of polyA+ RNA content by the keratinocyte statuses; differentiated, activated, senescent and immortalized. Four types of human keratinocyte samples represented these cell statuses: epidermal tissue (split-thickness skin grafts; SGs), cultured primary KCs in early and late passages, and HaCaT cell line. To reduce the sample size and sequencing costs and to control the fluctuation of mRNA concentration, we applied single-cell tagged reverse transcription (STRT) sequencing method for expression profiling using 10 ng of total RNA per sample which is ten times less than required for a conventional RNA-seq method [15]. For accurate expression profiling and statistical tests, we employed STRT RNA-seq with synthetic polyA+ spike-in RNA [16], and SAMstrat statistical package with spike-in based normalization [14]. We first evaluated the improvements of our approach on the genome-wide expression profiling and confirmed the accuracy of the improved methods by literature survey of the keratin and collagen genes. Then we extracted genes that correlated with the sample types, and genes contributing to the sample classification, especially transcription factors [17] and long noncoding RNAs [18], as candidate regulators for keratinocyte characters. These results provide new insights into the skin transcriptome and into the usefulness of primary KCs and HaCaTs as model systems.

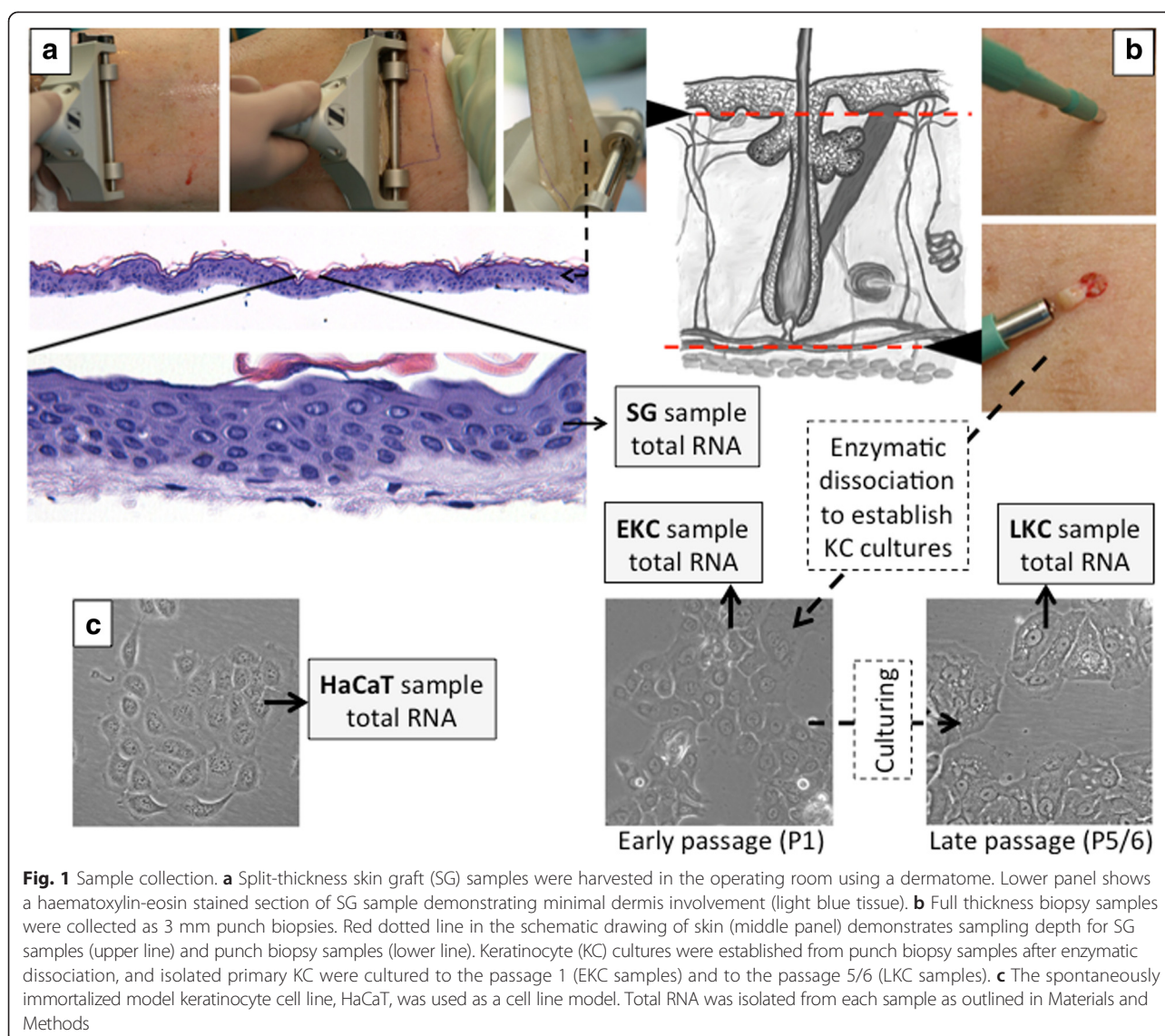
Results and discussion

Sample preparation, STRT RNAseq, and quality control

The protocol for sample preparation is depicted in Fig. 1. We collected SG biopsies with minimal inclusion of dermis and full thickness skin biopsies for KC culture from 8 donors undergoing plastic surgery (Additional file 1: Table S1). The SG samples were used directly for total RNA extraction whereas the full-thickness biopsies were used to set up KC cultures from which total RNA was extracted at early (1st; EKC) and late (5th–6th; LKC) passages. After RNA quality control (Additional file 2: Table S2), 16 samples were used to prepare two STRT libraries using 3 technical replicates, each containing 10 ng total RNA (Additional file 3: Table S3). Each STRT library was sequenced on four lanes of Illumina HiSeq 2000 instrument. In average, there were 10.8 million STRT reads and 7.92 million mapped reads per replica. After alignment to the human genome and gene-based quantitation, we confirmed consistency between all technical replicates (Additional file 4: Table S4, Additional file 5: Figure S1 and Additional file 6: Figure S2). One sample (10k1b, EKC replica 2 of donor 10k) exhibited exceptionally high relative polyA+ transcript counts (Additional file 5: Figure S1), and displayed unexpected overexpression of some abundantly expressed genes (Additional file 6: Figure S2). Therefore, we excluded it from further consideration as an outlier potentially biasing further analyses.

Varying polyA+ RNA content in 10 ng total RNA

A common assumption is that cells to be compared contain equal amounts of RNA. However, KCs have been shown to change their RNA content over time in long-term culture [13], leading us to further investigate the differences in polyA+ RNA contents in our samples. We found that the estimated polyA+ RNA contents as quantified against the added spike-in RNA controls varied in different sample types (Additional file 5: Figure S1). The variation was larger than the variation of the repeatedly measured total RNA amounts that were loaded for sequencing (Fig. 2a). Such differences can lead to the misinterpretation of differential expression when traditional endogenous gene-based normalization is applied. This is demonstrated in Fig. 2b, which is a comparison of 10k donor samples between SG and EKC. The endogenous gene-based normalization method did not estimate the spike-in levels equivalently although the amount of spike-in RNAs were equal in all samples. Because the normalized spike-in levels must be same in the comparison, we employed the recently developed normalization method, SAMstrat [14], which uses exclusively the spike-in RNAs for normalization (Fig. 2c). Validation assays by qRT-PCR confirmed the upregulation of two house-keeping genes, *RPLP0* and *RPL13A*, as predicted by the spike-in-based normalization, both of which were



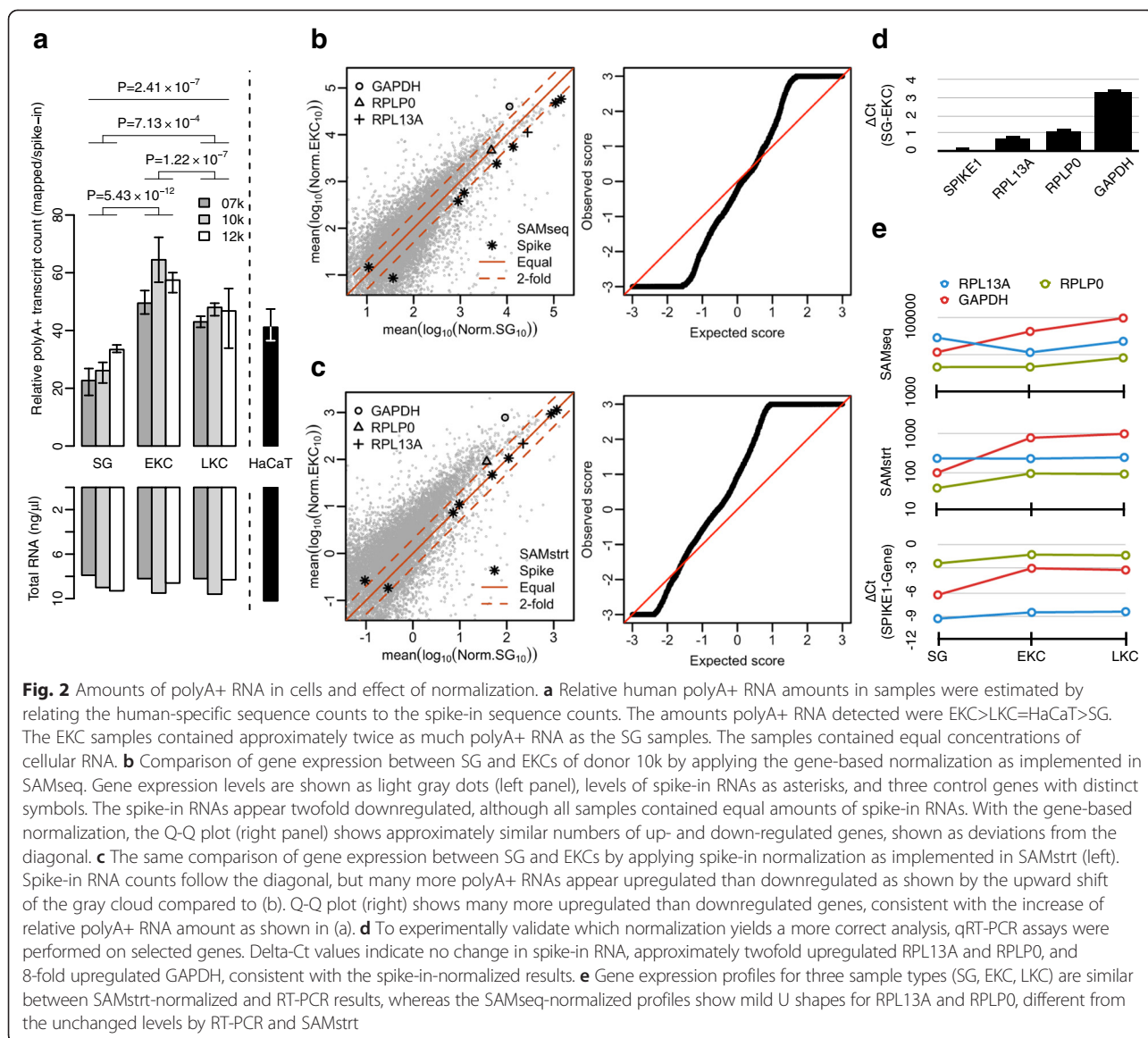
predicted unchanged or downregulated by the gene-based normalization (Fig. 2d). Moreover, the spike-in-based normalization method provided more consistent expression patterns in multiple samples with the qRT-PCR measurements (Fig. 2e). In conclusion, the observed variation in the polyA⁺ RNA content in 10 ng total RNA led to a misinterpretation of the expression pattern by the gene-based normalization method, but it became more reliable by the spike-in based normalization.

Characterization of SGs, cultured KCs, and HaCaTs by differentially expressed genes

When we assessed the transcriptome profiles in the different samples, we found 11,908 differentially expressed genes (Additional file 7: Table S5). Among them, 40 out of 58 cytokeratin genes were differentially expressed (Fig. 3a), and many of them well known markers for the

KC differentiation status both in cell culture and in tissue [1, 19, 20]. Hierarchical clustering confirmed significant contrasts between three sample types: SG, cultured KC and HaCaT. SGs contained several cytokeratin transcripts corresponding to cells at differentiated or differentiating epidermal layers (*KRT1*, 2, and 10), whereas the KCs contained cytokeratins typical of cells that maintain their proliferative capacity (*KRT5* and 14) or that are activated by wound healing, hyperproliferative skin diseases or in vitro culturing (*KRT6*, 16, and 17) [1, 20]. *KRT8* and *KRT18* that are the developmentally first keratins absent from normal skin and rather characterizing simple epithelia are in our data expressed by both cultured KCs and HaCaTs supporting their proliferative and undifferentiated nature [20].

There were no significant differences between the early (EKC) and late (LKC) passage KCs in the cytokeratin



levels. In contrast, HaCaT was remarkably different from both SGs, EKC and LKC expressing higher levels of cytokeratins 4, 13, 15, 19 and 81 (*KRT4, 13, 15, 19* and *81*). Furthermore, several cytokeratins (*KRT7, 8, 18, and 19*) characterising HaCaT by the spike-in normalization (Fig. 3a) were consistent with published protein expression patterns, low expression in skin, but high in HaCaT [21]. This observation was only partially supported by the gene-based normalization (Additional file 8: Figure S3) – by that method *KRT7* and *8* did not reach significant difference, suggesting that the gene-based normalization was less sensitive or less accurate than the spike-in normalization.

To further confirm the sample classification by STRT results, we compared the sample specific expression of different collagen genes (Fig. 3b), which have previously

characterized expression profiles in different types of tissues [22, 23]. 25 out of 44 collagen genes were differentially expressed. SGs expressed mainly connective tissue specific collagens (types I, V and VI), consistent with the presence of thin connective tissue layer underlying the epidermis, whereas cultured cells were characterized by the basement membrane (types IV) and skin hemidesmosome (type XVII) specific collagens again supporting the proliferative nature typical for the KCs in basal layer of epidermis.

Characterization of SGs, EKC, LKCs, and HaCaTs by coregulated genes

We approached the question how comparable cultured cells are as model systems for intact skin by elucidating the gene expression differences between the samples.

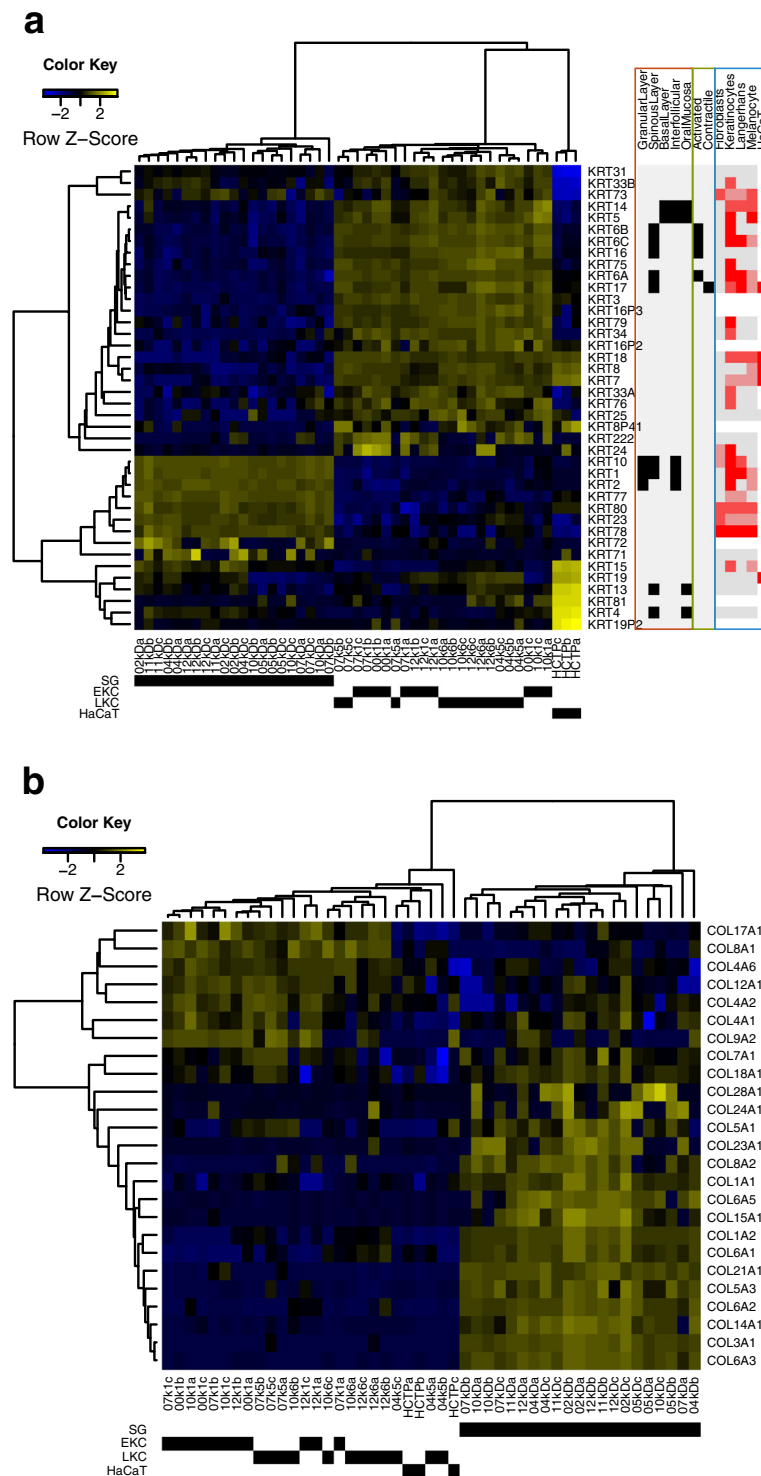


Fig. 3 Differential expression between the SGs, cultured KCs and HaCats. **a** The heat map panel to the left shows the expression of cytokeratins in different samples. Annotations for cytokeratins in the panel to the right for the gene expression on different layers and tissue types (orange) are based on Takahashi et al. [19], for the status in activation cycle (green) are based on Freedberg et al. [1], and for the protein expression in five cell types (blue) are based on Human Protein Atlas, HPA [21]. According to HPA, white denotes no data, gray means not detected (primary cell types) or with negative intensity (HaCaT), and red represents varying protein levels according to the intensity of the colour. SG, Split-thickness skin graft; EKC, early passage keratinocyte; LKC, late passage keratinocyte; HCTP, HaCaT. **b** The heat map shows the expression of collagens in different samples

We applied Principal Component Analysis (PCA; Fig. 4) to decompose the differences into several dimensions and to simplify the complexity of our dataset. PCA enabled multiclass comparisons between samples and improved the interpretation of expression profiles. The first principal component (PC), that depicts the largest variation between samples, classified the SGs as a separate group compared to the other samples. The second and third PCs separated the early and late passages of KCs from HaCaTs, respectively. In the following paragraphs, we interpret the meaning of each PC axis with literature surveys to assess appropriateness of the sample classifications based on our expression profile, and to decode insights into the differentiation and the growth control.

PC1 demonstrates the contrast between SGs and other sample types

First, we extracted genes correlating with the PC1. In this component, positively correlated genes referred to those with higher expression in the SGs when compared to KCs or HaCaTs, and negatively correlated genes acting oppositely. Our data showed that 3,402 genes correlated positively with the PC1 and thus were expressed higher in SGs (Table 1a and Additional file 9: Table S6), although the total polyA+ content of SGs was lower than that of KCs and HaCaTs. In contrast, 4,663 genes correlated negatively (Table 1a and Additional file 9: Table S6). Nine out of ten most upregulated genes in the SGs were previously associated with epidermal differentiation or with small organelles in differentiating cells (Table 1a), and five of ten most upregulated genes in KCs and HaCaTs were annotated as localized in mitochondria (Table 1b), which are lost from keratinocytes during epidermal differentiation [24]. To conclude, the most correlated known genes contributing to PC1 were thus consistent with the biological phenotype of the contrasted cell types.

To further interpret the PC1 and to find the associations between genes and phenotypes contrasted on PC, we performed gene set enrichment analysis amongst all genes that correlated with that PC (PC-GSEA). Our results showed that 136 out of 7,801 gene sets correlated positively, being upregulated in the SGs (q-value FDR < 1 %; Additional file 10: Table S7). The most significant gene set (Table 2a) was target genes of p53 and p63, which are known mediators of keratinocyte differentiation [25]. Similarly, 1,340 gene sets showed negative correlation (q-value FDR < 1 %; Additional file 10: Table S7). The 2nd, 4th, 6th, 9th, and 10th of significant gene sets (Table 2b) were related to mitochondria. Therefore, the PC-GSEA extracted meaningful contrasts of the biological functions and the phenotypes to interpret the PC1.

Since the PC scores representing the functions and phenotypes were calculated by linear combination of the expression profile and the loading coefficients, genes with large loading coefficients on each PC would be the key regulators for the functional contrast. For example, in case of PC1, genes with high positive loading coefficients contribute to the characteristic phenotypes and functions of SGs, and conversely, genes with high negative loading coefficients contribute to common characteristic phenotypes and functions of HaCaTs and KCs. When we extracted genes contributing to PC1, 223 genes showed positive loading and 104 genes showed negative loading (three sigma; Additional file 11: Table S8). 12 of the 223 positively contributing genes that explain the functions in SGs, and one of the 104 negative ones, characterizing the cultured cells, were known transcription factors (Fig. 5a; the definition of a transcription factor was based on [26]). Six of the 12 transcription factors upregulated in SGs were known regulators for skin maturation and differentiation phenotypes (Table 3). As an example, *POU2F3* (a.k.a. *Skn-1a/Oct11*) is a known transactivator of the suprabasal layer marker *KRT10* [27], which correlated positively

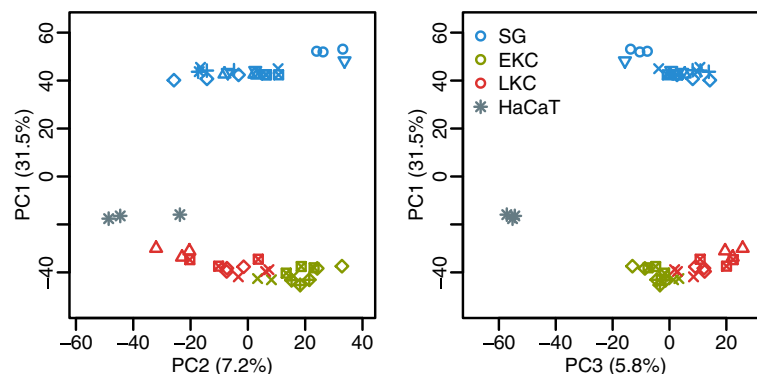


Fig. 4 Sample classification by the principal component analysis. PCA scatter plots using the spike-in normalized gene expression profiles. PC1 demonstrates the contrast between SGs and other sample types, PC2 depicts the contrast between EKC and HaCaTs, and PC3 shows the contrast between HaCaTs and LKCs. Percentages beside of the axis labels are the contribution ratios. Identical symbols between SGs and KCs denote identical donors in three technical replicas each. SG, Split-thickness skin graft; EKC, early passage keratinocyte; LKC, late passage keratinocyte

Table 1 Ten most correlated genes with PC1. Tables a and b are subsets of significantly correlated genes with relevant functions in skin lineage (for full data, see Additional file 9: Table S6). a Positively correlated genes, which were upregulated in SGs, and (b) negatively correlated genes, which were upregulated in KCs and HaCaTs

Gene Symbol	Score	Local FDR	
(a)			
RAB11FIP1	0.934	0.00044	
KRT80	0.933	0.00045	Localization around desmosomal plaques in earlier stages of differentiation [PMID:20843789]
ID4	0.915	0.00052	Lack of the protein in parakeratotic cells at upper skin layer [PMID:21663940]
PPL	0.911	0.00053	A component of desmosomes and of the cornified envelope [PMID:9412476]
KRT1	0.911	0.00054	Specifically expressed in the spinous and granular layers [PMID:10511477]
BCL6	0.900	0.00058	Expression at the terminal differentiation stage [PMID:8912662]
ERBB3	0.897	0.00059	Skin biopsy expressed more than the cultured cells [PMID:11571634]
PLAC2	0.896	0.00059	lncRNA controlling terminal differentiation [PMID:23201690]
PKP1	0.896	0.00059	Localization around desmosomal plaques and nuclei [PMID:16632867]
KRT10	0.894	0.00060	Specifically expressed in the spinous and granular layers [PMID:10511477]
(b)			
PRDX3	-0.922	0.00044	Mitochondrial [PMID:17893648]
SEC61G	-0.914	0.00045	
NDUFB3	-0.914	0.00052	Mitochondrial [PMID:12611891]
FXC1	-0.913	0.00053	Mitochondrial [PMID:14726512]
ATP5J	-0.911	0.00054	Mitochondrial [PMID:12110673]
GNG10	-0.911	0.00058	
TXNDC9	-0.911	0.00059	
MRPS23	-0.910	0.00059	Mitochondrial ribosomal protein
ENY2	-0.910	0.00059	
PSMB2	-0.909	0.00060	

with PC1 (Score = 0.89, local-FDR = 6.00×10^{-4}), and is also a known repressor for the basal layer marker *KRT14* [28], which correlated negatively with PC1 (Score = -0.68, local-FDR ~ 0). To conclude, differentiation and the mitochondrial phenotypes are possible interpretations of the PC1 and can be explained by the fluctuation of transcription factors that were clearly associated to sample types.

PC2 depicts the contrast between EKC and HaCaTs

PC2 captured the second largest variation which mostly shows the contrast between HaCaTs and EKC, with intermediate LKCs (Fig. 4). Three thousand nine hundred sixty nine genes correlated positively with PC2 and were thus expressed at higher level in EKC (Additional file 9: Table S6), and six of the top 10 positively correlated genes were polyA+ RNA binding proteins (Table 4). In contrast, there were no negatively correlated genes that would appear upregulated in HaCaT, which may depend on the fact that HaCaTs and LKCs had less polyA+ RNA than EKC (Fig. 2a). Accordingly, PC-GSEA towards PC2 revealed 23 positively correlating and only two negatively correlating

gene sets (Table 5 and Additional file 10: Table S7). When we investigated associations in the correlating genes and the gene sets as an interpretation of PC2, we found that the PC2 explained the difference of G1/S-transition between the EKC and HaCaTs both through negative and positive correlation. First, the genes that bear H3K27me3 in ES cells and have high-CpG-density promoter, showed negative correlation (i.e. upregulation in HaCaTs; MIKKELSEN_ES_HCP_WITH_H3K27ME3; q-value FDR ~ 0) [29]; the genes with H3K27me3 marks have actually been shown to be transcribed at G1/S- and S-phases in HaCaTs. Second, target genes of *RB1*, which is known to be negative regulator of the S-phase entry, showed positive correlation (i.e. upregulation in EKC; EGUCHI_CELL_CYCLE_RB1_TARGETS, q-value FDR = 4.76×10^{-3}) [30].

Then we proceeded to find genes that are the key regulators for the functional contrast on PC2. 137 genes showed high positive loading to PC2, and 111 genes showed negative loading (three sigma; Additional file 11: Table S8). Among them, five positive loading genes and nine negative ones were transcription factors (Fig. 5a).

Table 2 Ten most significant gene sets enriched in PC1 correlating genes. Tables a and b are subsets of gene sets that were significantly (FDR q-value < 1 %) enriched in PC1 correlating genes by PC-GSEA (for full data, see Additional file 10: Table S7). (a) Gene sets in positively correlated genes, which were upregulated in SGs, and (b) gene sets in negatively correlated genes, which were upregulated in KCs and HaCaTs. SIZE is number of genes belonging the gene set. NES is normalized enrichment score

Name	SIZE	NES	FDR q-val
(a)			
PEREZ_TP53_AND_TP63_TARGETS	198	2.967	0
SMID_BREAST_CANCER_NORMAL_LIKE_UP	449	2.908	0
BOQUEST_STEM_CELL_CULTURED_VS_FRESH_DN	31	2.774	0
KRAS.LUNG_UP.V1_DN	128	2.774	0
ABATES_COLORECTAL_ADENOMA_DN	248	2.760	0
WU_SILENCED_BY_METHYLATION_IN_BLADDER_CANCER	53	2.758	0
PEREZ_TP63_TARGETS	334	2.742	0
WINNEPENNINGCKX_MELANOMA_METASTASIS_DN	46	2.735	0
KEGG_ASTHMA	23	2.689	0
KEGG_ALLOGRAFT_REJECTION	33	2.663	0
(b)			
YAO_TEMPORAL_RESPONSE_TO_PROGESTERONE_CLUSTER_13	172	3.060	0
MOOTHA_VOXPHOS	86	3.038	0
WONG_EMBRYONIC_STEM_CELL_CORE	332	3.028	0
REACTOME_RESPIRATORY_ELECTRON_TRANSPORT_ATP_SYNTHESIS_BY_CHEMIOSMOTIC_COUPLING_AND_HEAT_PRODUCTION_BY_UNCOUPLING_PROTEINS_	81	3.016	0
FOURNIER_ACINAR_DEVELOPMENT_LATE_2	276	3.005	0
KEGG_OXIDATIVE_PHOSPHORYLATION	111	2.954	0
PENG_LEUCINE_DEPRIVATION_DN	186	2.947	0
GSE22886_UNSTIM_VS_IL15_STIM_NKCELL_DN	199	2.947	0
WONG_MITOCHONDRIA_GENE_MODULE	216	2.943	0
REACTOME_RESPIRATORY_ELECTRON_TRANSPORT	65	2.924	0

Interestingly, the positive loading genes *APBB1* [31], *ESPL1* [32], *TCF19* [33] and *ZNF300* [34] were known cell cycle regulators or contributors to cell proliferation. Moreover, one of the 137 positive loading genes and seven of the 111 negative ones were known lncRNAs (Fig. 5b). *UCA1* was a negatively loading lncRNA, known as essential for bladder cancer cell proliferation via CREB-dependent pathway [35]. Interestingly, Cyclin D1 expression in KCs is also under the CREB-dependent pathway [36]. In conclusion, the difference of G1/S-transition between HaCaTs and EKC is a possible interpretation for PC2, and again the fluctuation of transcription factors was highly associated to sample types.

PC3 shows the contrast between HaCaTs and LKCs

PC3 associated mostly with the variation between HaCaTs and LKCs (Fig. 4). We could not detect positively correlated genes (upregulated in LKC) with PC3, although these samples had equivalent polyA+ RNA contents

(Fig. 2a). In contrast, 2,992 correlated negatively referring to upregulation in HaCaT (Additional file 9: Table S6), and five of the top 10 negatively correlated genes codes polyA+ RNA binding protein (Table 6). In PC-GSEA, only 30 gene sets correlated positively with PC3, whereas 241 correlated negatively (Additional file 10: Table S7). As the interpretation of PC3, we found that it was associated with senescence, in accordance of KC senescence that does not apply to the continuously proliferating HaCaT cells. One explaining component was the positive correlation (upregulation in LKCs) of potassium channel genes (Table 7a). Potassium channel activation inhibits proliferation by activating a senescence program in breast cancer [37], and the G0/G1-arrest is accompanied by this activation. Consistently, not only the genes for G0 and early G1 phases, but also the other cell cycle associated genes were downregulated in LKCs (Table 7b). Furthermore, *miR-192* and *miR-34* target genes were upregulated in HaCaTs (negative correlation with PC3; Table 7c).

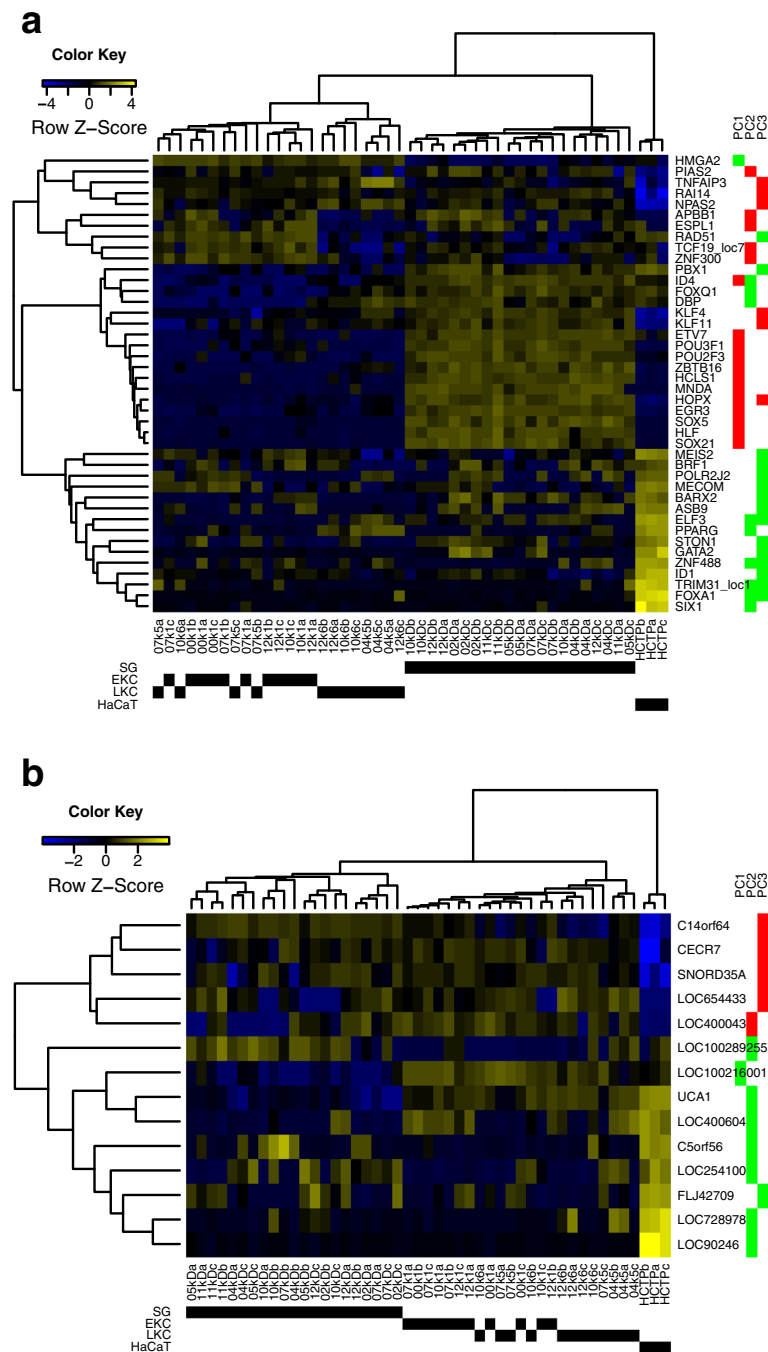


Fig. 5 Hierarchical clustering of expression profiles of high loading loci contributing to the sample classification for PC1, PC2 and PC3. Panel (a) shows transcription factors (TFs) in the high loading profiles of features, and panel (b) known noncoding genes. The expression of different TFs separates SGs, KCs and HaCaTs from each other whereas the expression of noncoding genes mainly separates HaCaTs from other samples. The contribution to the three first PCs is shown to the right red denoting positively contributing genes and green denoting negatively contributing genes. SG, Split-thickness skin graft; EKC, early passage keratinocyte; LKC, late passage keratinocyte; HCTP, HaCaT

Those miRNAs are functionally associated with p53-dependent cellular maintenance and aging (miR-34 [38, 39], and miR-192 [40, 41]).

We next attempted to find supporting genes for this interpretation. A total of 117 genes showed high positive

loading to PC3, and 144 genes showed high negative loading (three sigma; Additional file 11: Table S8). Among them, six positive and 15 negative loading genes were transcription factors (Fig. 5a). One negatively loading (upregulated in HaCaTs) gene was *RAD51*, known to be

Table 3 Transcription factors, positively contributing to PC1. Table shows a subset of significantly contributing loci with relevant functions in skin lineage (for full data, see Additional file 11: Table S8)

Gene Symbol	Loading	Z-score	
HLF	1.059	3.690	Inhibitor of cell death response [PMID:23415677]
ZBTB16	1.039	3.621	
HOPX	1.022	3.558	Controlling differentiation-dependent genes [PMID:20226564]
EGR3	0.999	3.477	
ID4	0.986	3.436	Lack of the protein in parakeratotic cells at upper skin layer [PMID:21663940]
MNDA	0.968	3.369	
HCLS1	0.947	3.297	
SOX5	0.947	3.295	Genes coding SOX5 binding sites at the promoters were PC1 positive correlation (V_{SOX5_01} ; q-value FDR ~ 0)
SOX21	0.937	3.261	Master regulator of hair shaft cuticle differentiation [PMID:19470461]
ETV7	0.928	3.227	
POU3F1	0.920	3.200	Transactivator for FLG (a.k.a. profilaggrin; PC1 positive correlation, Local- FDR = 7.34×10^{-4} ; [PMID:10809764])
POU2F3	0.906	3.151	10-4; [PMID:10809764] & [PMID:7682011]); repressor for KRT14 (PC1 negative correlation, Local-FDR ~ 0 ; [PMID:11429405])

involved in the homologous recombination and the repair of DNA. Expression of *RAD51* is regulated by Lamin A (*LMNA*) [42], and expression of the *LMNA* was consistently negatively correlated (Local-FDR = 8.99×10^{-4}). It's well known that the mutations of *LMNA* lead to Hutchinson–Gilford progeria syndrome characterized by a premature aging [43]. Therefore, senescence and cellular aging responses would be a possible interpretation for PC3.

Conclusion

STRT RNA-seq method complemented with synthetic RNAs revealed a variation of polyA+ RNA content per total RNA in different cell types, SGs, EKC, LKCs and HaCaTs, reflecting the activity of the cell type. Even though

the STRT reads are concentrated towards the 5' end of the polyA+ transcripts and the method has limited resolution at 2nd and more downstream exons, the advantages of the method include the small amount of starting material needed for library preparation, early multiplexing of up to 92 samples reducing the cost and time of library preparation, and the inclusion of external spike-in RNAs as a standard procedure. The spike-in normalization has been shown to be a valuable tool when comparing samples with fluctuating polyA+ RNA contents [14, 44]. We showed that the use of spike-in-based normalization produced consistent results with qPCR validations, and provided us with deeper insights into KC biology. In contrary, the traditional gene-based normalization method led to inaccurate expression profiles. Moreover, our approach would be applicable not only for the studies on KCs but also for the other studies with fluctuation of polyA+ RNA content, for example those on single cells with different types or sizes [45, 46].

We applied PCA to elucidate dissimilarity between the samples, and also to decompose the differences. The three first PCs represented differentiation and the mitochondrial phenotypes between SGs and cultured cells, G1/S-transition between HaCaTs and EKC, and senescence and cellular aging responses between HaCaTs and LKCs. All cultured cells differed from tissue samples and HaCaT cells differed remarkably from other cultured cells based on both PCA and the comparison of previously known KC markers, cytokeratins. Our results thus suggest that great caution should be paid when using cultured primary KCs and cell models like HaCaTs as models for skin, especially when focusing on the pathways revealed by PCA. The transcriptomes of cultured primary KCs and HaCaTs resemble that of activated skin rather than normal skin as shown also by others [10, 11].

Table 4 Ten most positively correlated genes with PC2. Table is a subset of positively correlated genes with PC2, and the thick mark indicates if the gene codes polyA+ RNA binding protein (for full data, see Additional file 10: Table S6)

Gene symbol	Score	Local FDR	polyA + RNA binding [PMID: 22658674]
HNRNPH1	0.855	0.00000	✓
SCAF11	0.829	0.00002	✓
HNRNPA3	0.823	0.00003	✓
BCLAF1	0.802	0.00008	✓
OXCT1	0.800	0.00008	✓
ODF2L	0.798	0.00008	✓
HNRNPAB	0.789	0.00010	✓
PNN	0.788	0.00011	✓
UBE2G2	0.787	0.00011	✓
SPARC	0.787	0.00011	✓

Table 5 Most significant gene sets enriched in PC2 correlating genes. (a) Table is a subset of gene sets (ten out of 23) significantly (FDR q-value < 1 %) enriched in PC2 positively correlating genes, which were upregulated in EKC, by PC-GSEA (for full data, see Additional file 10: Table S7). (b) Table is gene sets significantly enriched in PC2 negatively correlating genes, which were upregulated in HaCaTs. SIZE is number of genes belonging the gene set. NES is normalized enrichment score

Name	SIZE	NES	FDR q-val
(a)			
PUJANA_BRCA_CENTERED_NETWORK	117	1.909	0.00492
ZHANG_TLX_TARGETS_UP	89	1.875	0.00885
BURTON_ADIPOGENESIS_PEAK_AT_16H	40	1.873	0.00590
PUJANA_XPRSS_INT_NETWORK	168	1.869	0.00467
ZHANG_TLX_TARGETS_36HR_DN	185	1.868	0.00394
EGUCHI_CELL_CYCLE_RB1_TARGETS	23	1.856	0.00476
REACTOME_TRANSPORT_OF_MATURE_TRANSCRIPT_TO_CYTOSOL	52	1.846	0.00436
ABRAMSON_INTERACT_WITH_AIRE	44	1.845	0.00394
GOLUB_ALL_VS_AML_UP	24	1.841	0.00383
ZHANG_TLX_TARGETS_60HR_DN	275	1.839	0.00374
(b)			
MIKKELSEN_ES_HCP_WITH_H3K27ME3	35	2.441	0.00000
REACTOME_XENOBIOTICS	15	2.345	0.00851

In this study, we present an approach to compare highly varying cell types by applying synthetic RNA based normalization. For further studies or applications of other biological events, the key is to find the hidden associations between genes and phenotypes which are contrasted on PCs. We also note that there are still many poorly annotated genes in the genome that might

Table 6 Ten most negatively correlated genes with PC3. Table is a subset of negatively correlated genes with PC3, and the thick mark indicates if the gene codes polyA+ RNA binding protein (for full data, see Additional file 9: Table S6)

Gene symbol	Score	Local FDR	polyA + RNA binding [PMID: 22658674]
PRPF8	-0.885	0.00006	✓
APOL6	-0.826	0.00018	
CCDC15	-0.826	0.00018	
TTF1	-0.823	0.00019	
ZC3H11A	-0.813	0.00021	✓
NUCKS1	-0.809	0.00021	✓
PCBP2	-0.808	0.00021	✓
H2AFV	-0.804	0.00022	
RBBP7	-0.500	0.00023	
HMG2	-0.798	0.00023	✓

be revealed by our approach. Moreover, PCA without sample pre-classification might be applied in studying gene expression in complex disorders using a large enough cohort.

Methods

Sample collection, cell culture, RNA extraction, and STRT RNA-seq

All subjects involved in this study provided written informed consent under a protocol adherent to the Helsinki Guidelines and approved by the Institutional Review Board of the Helsinki University Central Hospital.

Split-thickness skin grafts (SGs) were harvested as outlined previously [47]. Briefly, SG samples were obtained using a compressed air-driven dermatome (Zimmer®, Warsaw, IN) with a fixed thickness setting of 2/1000 in. to obtain a representative sample of epidermis to its full thickness with minimal dermis involvement from the donor site skin. In order to initiate keratinocyte cultures, full thickness skin samples (3-mm diameter punch biopsies) were collected (Additional file 1: Table S1). The quality of SG samples was examined from HE-stained paraffin sections. The SGs were immediately immersed in RNAlater to ensure the least possible manipulation and gene expression changes.

Epidermal cells were isolated from the full thickness skin with dispase digestion followed by trypsinization to enable collection of all primary cell types and phenotypes of the epidermis in the initial harvest. Human primary keratinocytes were cultured in Keratinocyte Growth Medium 2 (PromoCell # C-20011) with calcium (0.06 mM) and PromoCell supplements (#C-39016). Cell culture dishes were coated with collagen I (Gibco Rat tail, A-10483-01). Cells were routinely passaged, and samples were collected from early (passage 1; EKC) and late passages (passage 5 or 6; LKC). The human immortalized keratinocyte HaCaT cell line was grown in low glucose DMEM (Lonza) supplemented with 5 % FBS, 2 mM L-glutamine, 1 mM sodium pyruvate solution, 0.1 mM non-essential amino acids, 100 U/ml penicillin and 100 µg/ml streptomycin at 37 °C and 5 % CO₂. HaCaT cells were collected at passage 43 for RNA isolation.

Total RNA was extracted by miRNeasy kit (Qiagen) from both tissue samples and cells. RNA concentrations were measured by Nanodrop and Qubit and the quality was controlled by Bioanalyzer (RIN for all samples >8; Additional file 2: Table S2).

STRT RNA-seq

Qualified total RNA samples (10 ng of each replicate, three replicates for each sample) were used for RNA sequencing library preparation according to the STRT protocol [16], which was adjusted for 10 ng samples by decreasing the number of cycles to 10 during the

Table 7 Significant gene sets enriched in PC3 correlating genes. Tables a, b and c are subsets of gene sets significantly (FDR q-value < 1 %) enriched in PC3 correlating genes by PC-GSEA (for full data, see Additional file 10: Table S7). (a) Table is a subset of the ten (out of 30) gene sets most significantly enriched in the positively correlating genes, which were upregulated in LKCs. (b) Table is cell cycle associated gene sets significantly enriched in the negatively correlating genes, which were upregulated in HaCaTs. (c) Table is miRNA-target gene sets significantly enriched in PC3 negatively correlating genes. SIZE is number of genes belonging the gene set. NES is normalized enrichment score

Name	SIZE	NES	FDR q-val
(a)			
REACTOME_OLFACTORY_SIGNALING_PATHWAY	36	2.967	0
DAZARD_UV_RESPONSE_CLUSTER_G28	20	2.908	0
DAZARD_UV_RESPONSE_CLUSTER_G24	27	2.774	0
PID_CONE_PATHWAY	16	2.774	0
MAHADEVAN_RESPONSE_TO_MP470_DN	19	2.760	0
WANG_TNF_TARGETS	23	2.758	0
BURTON_ADIPOGENESIS_1	33	2.742	0
AMIT_EGF_RESPONSE_60_MCF10A	38	2.735	0
VOLTAGE_GATED_POTASSIUM_CHANNEL_COMPLEX	29	2.689	0
RORIE_TARGETS_OF_EWSR1_FLI1_FUSION_UP	30	2.663	0
(b)			
REACTOME_G2_M_CHECKPOINTS	41	1.865	0.00029
REACTOME_MITOTIC_PROMETAPHASE	85	1.822	0.00064
REACTOME_MITOTIC_M_M_G1_PHASES	167	1.783	0.00114
REACTOME_G0_AND_EARLY_G1	23	1.732	0.00241
REACTOME_CELL_CYCLE	392	1.710	0.00314
REACTOME_CELL_CYCLE_CHECKPOINTS	111	1.690	0.00428
REACTOME_S_PHASE	106	1.660	0.00596
REACTOME_M_G1_TRANSITION	78	1.646	0.00706
REACTOME_REGULATION_OF_MITOTIC_CELL_CYCLE	77	1.621	0.00908
(c)			
GEORGES_CELL_CYCLE_MIR192_TARGETS	62	1.726	0.00272
TOYOTA_TARGETS_OF_MIR34B_AND_MIR34C	449	1.675	0.00501

first PCR amplification. The libraries (Additional file 3: Table S3) were sequenced using an Illumina HiSeq 2000 instrument. Preprocessing of STRT reads, alignments and per-gene quantitation were performed by an established analysis pipeline [16]. Differential expression analysis was performed by SAMstrt [14], and also by SAMseq [48] for an example of the gene-based normalization. Differentially expressed genes by the four sample types were extracted by multiclass response test; threshold of the significantly regulated genes is Local-FDR < 1 %. Gene type (e.g. protein coding, pseudo, noncoding), genes of glycolysis/gluconeogenesis and transcription factors were classified based on Entrez Gene, KEGG pathway [KEGG:hsa00010]

and Ravasi et al. [26], respectively. For cytokeratin expression analysis, we selected the gene symbols that begin “KRT” followed by number. We performed PCA with the scaling but non-centering preprocess steps. Correlation of gene expression with PC was estimated by SAMstrt quantitative response test. Scores of samples on a PC were given as the quantitative values, and threshold of the significantly correlated gene is Local-FDR < 1 %. PC-GSEA, which tests correlation of gene set with PC, was by GSEA [49] preranked test towards c1, c2, c3, c5, c6 and c7 of MSigDB version 4. The ranked lists contain the gene correlation scores estimated by SAMstrt as described above; threshold of the significantly correlated gene set is q-value FDR < 1 %.

qRT-PCR

The qualified total RNA samples 10kD, 10k1 and 10k6, which were used for sequencing with STRT method, were subjected to cDNA synthesis. Equal amount of the SPIKE-in RNA mix (ArrayControl RNA, AM1780M, Ambion) was added to each cDNA synthesis reaction according to the STRT-library preparation protocol described above. cDNA synthesis was carried out using oligo dT-primers and SuperScript III First-Strand synthesis system for RT-PCR (18080–151, Invitrogen) according to manufacturer’s instructions. 5 ng of cDNA was applied to each qPCR assay and each sample was run in three technical replicates. qPCR was carried out using an ABI PRISM 7500 Fast Real-Time PCR System with Fast SYBR® Green Master mix (4385617, both from Applied Biosystems) according to manufacturer’s instructions. The primer sequences are shown in Additional file 12: Table S9.

Availability of supporting data

The processed STRT reads supporting the results of this article are available in the European Nucleotide Archive (<http://www.ebi.ac.uk/ena/data/view/PRJEB8997>).

Additional files

Additional file 1: Table S1. Patients and the prepared samples.

Additional file 2: Table S2. The prepared samples and the total RNA qualities.

Additional file 3: Table S3. STRT library designs, sample notation and the sequencing summary. The sample name consists of 5 characters. The former 4 characters represent the sample type whether HaCaT cell line (HCTP) or the other primary samples as defined by patient and type identifiers in Additional file 2: Table S2. The last one character either a, b or c represent the technical replicates.

Additional file 4: Table S4. Similarity between technical replicates. The similarity was estimated by Pearson correlation coefficients of raw read counts.

Additional file 5: Figure S1. Variation of relative polyA+ transcript counts. There are three replicates (a, b and c from dark to bright filling colors) in each sample. The relative polyA+ transcript count was estimated by mapped read count per spike-in read count; we added the same amount of

polyA+ tailed spike-in RNAs into all 10 ng total RNA samples before the library synthesis. The ratio of the mapped reads on the reference human genome to the spike-in reads is a relative concentration of endogenous polyA+ RNAs in the 10 ng total RNA, which can be compared with the other samples. One outlier, 10k1b, was excluded for the further analysis as described in Additional file 6: Figure S2.

Additional file 6: Figure S2. Unexpected overexpression of some abundantly expressed genes in 10k1b. Scatter plots show comparisons of per-gene raw read counts between the technical replicas. (a) Comparisons in 07kD SGs as a reference. These replicas had the worst correlation coefficients (see also Additional file 4: Table S4). (b) Comparisons in 10k1 EKC. The comparisons with the replica b, especially between the replicas a and b, had broader scatter than one of replicas a vs. c and the 07kD replicas. The 10k1b is the only outlier in the replicas. Heat maps and the hierarchical clustering of significantly expressed cyokeratins (c) and glycolysis-gluconeogenesis (d) genes including the 10k1b replica. Some genes of the 10k1b were overrepresented, although the trends were similar.

Additional file 7: Table S5. Differentially expressed genes between the multiple classes. There are 11,908 unique genes in 12,246 (of 20,500) differentially expressed features. The columns from G to L are the statistical values estimated by SAMstr. Local Gene ID is usually identical with Gene Symbol except for multicopy genes, which have suffix “_loc” with numbers, and for repetitive elements, which have prefix “r_”. Entrez Gene ID and Gene Type are based on Entrez Gene. Glycolysis genes and Transcription Factors are denoted “GL” and “TF” at the columns E and F. Contrasts are the standardized mean difference of the gene expression between the four classes. Positive contrast means overexpression, and negative contrast the opposite.

Additional file 8: Figure S3. Hierarchical clustering of cyokeratin expression profiles with gene-based normalization. In the 11,689 differentially expressed genes by the gene-based normalization, 38 were known cyokeratin genes shown in this figure. The heat map panel to the left shows the expression of cyokeratins in different samples. Annotations for cyokeratins in the panel to the right for the gene expression on different layers and tissue types (orange) are based on Takahashi et al. [19], for the status in activation cycle (green) are based on Freedberg et al. [1], and for the protein expression in five cell types (blue) are based on Human Protein Atlas, HPA [21]. According to HPA, white denotes no data, gray means not detected (primary cell types) or with negative intensity (HaCaT), and red represents varying protein levels according to the intensity of the colour.

Additional file 9: Table S6. PC correlating loci. Sheet name indicates PC number and direction of the correlation. Each sheet contains significantly correlated loci (Local-FDR < 1 % by SAMstr quantitative response test towards the score of samples on the PC; the columns C and D are the statistical values). Local Gene ID is usually identical with Gene Symbol except for multicopy genes, which have suffix “_loc” and the copy number. There were no negatively correlating genes with PC2 and no positively correlating genes with PC3.

Additional file 10: Table S7. PC correlating gene sets. Sheet name indicates PC number and direction of the correlation. Each sheet contains significantly correlating gene sets (q-value FDR < 1 % by GSEA [49] with a gene list preranked by SAMstr quantitative response test towards the score of samples on PC).

Additional file 11: Table S8. PC contributing features. Sheet name indicates PC number and direction of the contribution. Each sheet contains significantly high contributing loci (three sigma). Local Gene ID is usually identical with Gene Symbol except for multicopy genes, which have suffix “_loc” and the copy number.

Additional file 12: Table S9. qRT-PCR primers.

Abbreviations

EKC: Cultured keratinocyte at early passage; GSEA: Gene set enrichment analysis; KC: Keratinocyte; LKC: Cultured keratinocyte at late passage; PC: Principal component; PCA: Principal component analysis; SG: Split-thickness skin graft; STRT: Single-cell tagged reverse transcription.

Competing interests

The authors declare that they have no competing interests.

Authors' contributions

SK analysed the data and wrote the first manuscript version. TS, AS, KN and MHT managed sample collection and processing. EMJ performed verification gene expression analyses, AJ library preparation and sequencing, and PL processed the raw sequences for the analysis. JV selected sample donors and performed surgical procedures. SL, OE, EK and JK supervised the project. All authors contributed to the editing of the manuscript. All authors read and approved the final manuscript.

Acknowledgements

We are indebted to late Professor Ulpu Saarialho-Kere with whom this study was conceived. We thank the anonymous donors for these studies, and Sari Suomela, Auli Saarinen, Pia Pekkanen, and Allii Tallqvist for expert help. This study was reviewed and approved by the ethics review board according to the applicable laws (Dnro 66/13/03/02/2010 in Helsinki). This work was in part supported by Swedish Research Council, Sigrid Jusélius Foundation and the Karolinska Institutet Distinguished Professor Award to JK; the Strategic Research Programme in Diabetes at Karolinska Institutet to JK and SK; TEKES to EK; Academy of Finland to OE; Helsinki University Central Hospital EVO funds to JV; the Jane & Aatos Erkko Foundation and the Instrumentarium Science Foundation to E-MJ; and Karolinska Institutet internal grants to SK (2013fobi38281 and 2013p4re39181). The computations were performed on resources provided by SNIC through Uppsala Multidisciplinary Center for Advanced Computational Science (UPPMAX) under Project b2010037.

Author details

¹Department of Biosciences and Nutrition, Karolinska Institute and Center for Innovative Medicine, Huddinge, Sweden. ²Folkhälsan Institute of Genetics, Helsinki, Finland. ³Department of Medical Genetics, Haartman Institute and Research Programs Unit, Molecular Neurology, University of Helsinki, Helsinki, Finland. ⁴Department of Pharmacology, Faculty of Medicine, University of Helsinki, Helsinki, Finland. ⁵Helsinki Burn Center, Helsinki University Central Hospital, University of Helsinki, Helsinki, Finland. ⁶Department of Medical Biochemistry and Biophysics, Karolinska Institutet, Stockholm, Sweden. ⁷Science for Life Laboratory, Solna, Sweden.

Received: 21 January 2015 Accepted: 29 May 2015

Published online: 25 June 2015

References

- Freedberg IM, Tomic-Canic M, Komine M, Blumenberg M. Keratins and the keratinocyte activation cycle. *J Invest Dermatol.* 2001;116:633–40.
- Blanpain C, Fuchs E. Epidermal homeostasis: a balancing act of stem cells in the skin. *Nat Rev Mol Cell Biol.* 2009;10:207–17.
- Simpson CL, Patel DM, Green KJ. Deconstructing the skin: cytoarchitectural determinants of epidermal morphogenesis. *Nat Rev Mol Cell Biol.* 2011;12:565–80.
- Rockwell GA, Johnson G, Sibatani A. In vitro senescence of human keratinocyte cultures. *Cell Struct Funct.* 1987;12:539–48.
- Boukamp P, Petrussevska RT, Breitkreutz D, Hornung J, Markham A, Fusenig NE. Normal keratinization in a spontaneously immortalized aneuploid human keratinocyte cell line. *J Cell Biol.* 1988;106:761–71.
- Lehman TA, Modali R, Boukamp P, Stanek J, Bennett WP, Welsh JA, et al. p53 mutations in human immortalized epithelial cell lines. *Carcinogenesis.* 1993;14:833–9.
- Boukamp P, Popp S, Altmeyer S, Hülsen A, Fasching C, Cremer T, et al. Sustained nontumorigenic phenotype correlates with a largely stable chromosome content during long-term culture of the human keratinocyte line HaCaT. *Genes Chromosomes Cancer.* 1997;19:201–14.
- Schoop VM, Mirancea N, Fusenig NE. Epidermal organization and differentiation of HaCaT keratinocytes in organotypic coculture with human dermal fibroblasts. *J Invest Dermatol.* 1999;112:343–53.
- FANTOM Consortium, Suzuki H, Forrest ARR, van Nimwegen E, Daub CO, Balwierz PJ, et al. The transcriptional network that controls growth arrest and differentiation in a human myeloid leukemia cell line. *Nat Genet.* 2009;41:553–62.
- Gazel A, Ramphal P, Rosdy M, De Wever B, Tornier C, Hosen N, et al. Transcriptional profiling of epidermal keratinocytes: comparison of genes

- expressed in skin, cultured keratinocytes, and reconstituted epidermis, using large DNA microarrays. *J Invest Dermatol.* 2003;121:1459–68.
11. Smiley AK, Klingenberg JM, Aronow BJ, Boyce ST, Kitzmiller WJ, Supp DM. Microarray analysis of gene expression in cultured skin substitutes compared with native human skin. *J Invest Dermatol.* 2005;125:1286–301.
 12. Jabbari A, Suárez-Fariñas M, Dewell S, Krueger JG. Transcriptional profiling of psoriasis using RNA-seq reveals previously unidentified differentially expressed genes. *J Invest Dermatol.* 2012;132:246–9.
 13. Staiano-Coico L, Higgins PJ, Darzynkiewicz Z, Kimmel M, Gottlieb AB, Pagan-Charry I, et al. Human keratinocyte culture. Identification and staging of epidermal cell subpopulations. *J Clin Invest.* 1986;77:396–404.
 14. Katayama S, Töhönen V, Linnarsson S, Kere J. SAMstr: statistical test for differential expression in single-cell transcriptome with spike-in normalization. *Bioinformatics.* 2013;29:2943–5.
 15. Illumina Inc, San Diego, CA, USA. TrueSeq RNA sample preparation V2 guide. 15026495 edition. Rev F. 2014. http://support.illumina.com/downloads/truseq_rna_sample_preparation_v2_guide_15026495.html.
 16. Islam S, Kjällquist U, Moliner A, Zajac P, Fan J-B, Lönnerberg P, et al. Highly multiplexed and strand-specific single-cell RNA 5' end sequencing. *Nat Protoc.* 2012;7:813–28.
 17. Eckert RL, Crish JF, Banks EB, Welter JF. The epidermis: genes on - genes off. *J Invest Dermatol.* 1997;109:501–9.
 18. Fatica A, Bozzoni I. Long non-coding RNAs: new players in cell differentiation and development. *Nat Rev Genet.* 2014;15:7–21.
 19. Takahashi K, Coulombe PA, Miyachi Y. Using transgenic models to study the pathogenesis of keratin-based inherited skin diseases. *J Dermatol Sci.* 1999;21:73–95.
 20. Fuchs E. Keratins and the skin. *Annu Rev Cell Dev Biol.* 1995;11:123–53.
 21. Uhlen M, Oksvold P, Fagerberg L, Lundberg E, Jonasson K, Forsberg M, et al. Towards a knowledge-based human protein atlas. *Nat Biotechnol.* 2010;28:1248–50.
 22. Simeone A, Acampora D, Mallamaci A, Stornaiuolo A, D'Apice MR, Nigro V, et al. A vertebrate gene related to orthodenticle contains a homeodomain of the bicoid class and demarcates anterior neuroectoderm in the gastrulating mouse embryo. *EMBO J.* 1993;12:2735–47.
 23. Myllyharju J, Kivirikko KI. Collagens, modifying enzymes and their mutations in humans, flies and worms. *Trends Genet.* 2004;20:33–43.
 24. Moriyama M, Moriyama H, Uda J, Matsuyama A, Osawa M, Hayakawa T. BNIP3 plays crucial roles in the differentiation and maintenance of epidermal keratinocytes. *J Invest Dermatol.* 2014;134:1627–35.
 25. Truong AB, Kretz M, Ridky TW, Kimmel R, Khavari PA. p63 regulates proliferation and differentiation of developmentally mature keratinocytes. *Genes Dev.* 2006;20:3185–97.
 26. Ravasi T, Suzuki H, Cannistraci CV, Katayama S, Bajic VB, Tan K, et al. An atlas of combinatorial transcriptional regulation in mouse and man. *Cell.* 2010;140:744–52.
 27. Andersen B, Schonemann MD, Flynn SE, Pearse RV, Singh H, Rosenfeld MG. Skn-1a and Skn-1i: two functionally distinct Oct-2-related factors expressed in epidermis. *Science.* 1993;260:78–82.
 28. Sugihara TM, Kudryavtseva EI, Kumar V, Horridge JJ, Andersen B. The POU domain factor Skin-1a represses the keratin 14 promoter independent of DNA binding. A possible role for interactions between Skn-1a and CREB-binding protein/p300. *J Biol Chem.* 2001;276:33036–44.
 29. Peña-Diaz J, Hegre SA, Anderssen E, Aas PA, Mjelle R, Gilfillan GD, et al. Transcription profiling during the cell cycle shows that a subset of Polycomb-targeted genes is upregulated during DNA replication. *Nucleic Acids Res.* 2013;41:2846–56.
 30. Sherr CJ, Roberts JM. CDK inhibitors: positive and negative regulators of G1-phase progression. *Genes Dev.* 1999;13:1501–12.
 31. Bruni P, Minopoli G, Brancaccio T, Napolitano M, Faraonio R, Zambrano N, et al. Fe65, a ligand of the Alzheimer's beta-amyloid precursor protein, blocks cell cycle progression by down-regulating thymidylate synthase expression. *J Biol Chem.* 2002;277:35481–8.
 32. Chestukhin A, Pfeffer C, Milligan S, DeCaprio JA, Pellman D. Processing, localization, and requirement of human separase for normal anaphase progression. *Proc Natl Acad Sci U S A.* 2003;100:4574–9.
 33. Krautkramer KA, Linnemann AK, Fontaine DA, Whillock AL, Harris TW, Schleis GJ, et al. Tcf19 is a novel islet factor necessary for proliferation and survival in the INS-1 β -cell line. *Am J Physiol Endocrinol Metab.* 2013;305:E600–10.
 34. Wang T, Wang X-G, Xu J-H, Wu X-P, Qiu H-L, Yi H, et al. Overexpression of the human ZNF300 gene enhances growth and metastasis of cancer cells through activating NF- κ B pathway. *J Cell Mol Med.* 2012;16:1134–45.
 35. Yang C, Li X, Wang Y, Zhao L, Chen W. Long non-coding RNA UCA1 regulated cell cycle distribution via CREB through PI3-K dependent pathway in bladder carcinoma cells. *Gene.* 2012;496:8–16.
 36. Hwang B-J, Utti C, Steinberg M. Induction of cyclin D1 by submicromolar concentrations of arsenite in human epidermal keratinocytes. *Toxicol Appl Pharmacol.* 2006;217:161–7.
 37. Lansu K, Gentile S. Potassium channel activation inhibits proliferation of breast cancer cells by activating a senescence program. *Cell Death Dis.* 2013;4:e652.
 38. Yamakuchi M, Lowenstein CJ. miR-34, SIRT1 and p53: the feedback loop. *Cell Cycle.* 2009;8:712–5.
 39. Antonini D, Russo MT, De Rosa L, Gorrese M, Del Vecchio L, Missero C. Transcriptional repression of miR-34 family contributes to p63-mediated cell cycle progression in epidermal cells. *J Invest Dermatol.* 2010;130:1249–57.
 40. Georges SA, Biery MC, Kim S-Y, Schelter JM, Guo J, Chang AN, et al. Coordinated regulation of cell cycle transcripts by p53-Inducible microRNAs, miR-192 and miR-215. *Cancer Res.* 2008;68:10105–12.
 41. Braun CJ, Zhang X, Savelyeva I, Wolff S, Moll UM, Schepeler T, et al. p53-Responsive micromRNAs 192 and 215 are capable of inducing cell cycle arrest. *Cancer Res.* 2008;68:10094–104.
 42. Redwood AB, Gonzalez-Suarez I, Gonzalo S. Regulating the levels of key factors in cell cycle and DNA repair: new pathways revealed by lamins. *Cell Cycle.* 2011;10:3652–7.
 43. Prokocimer M, Barkan R, Gruenbaum Y. Hutchinson-Gilford progeria syndrome through the lens of transcription. *Aging Cell.* 2013;12:533–43.
 44. Lovén J, Orlando DA, Sigova AA, Lin CY, Rahl PB, Burge CB, et al. Revisiting global gene expression analysis. *Cell.* 2012;151:476–82.
 45. Dobson AT, Raja R, Abeyta MJ, Taylor T, Shen S, Haqq C, et al. The unique transcriptome through day 3 of human preimplantation development. *Hum Mol Genet.* 2004;13:1461–70.
 46. Islam S, Kjällquist U, Moliner A, Zajac P, Fan J-B, Lönnerberg P, et al. Characterization of the single-cell transcriptional landscape by highly multiplex RNA-seq. *Genome Res.* 2011;21:1160–7.
 47. Nuutila K, Siltanen A, Peura M, Bizik J, Kaartinen I, Kuokkanen H, et al. Human skin transcriptome during superficial cutaneous wound healing. *Wound Repair Regen.* 2012;20:830–9.
 48. Li J, Tibshirani R. Finding consistent patterns: a nonparametric approach for identifying differential expression in RNA-Seq data. *Stat Methods Med Res.* 2013;22:519–36.
 49. Subramanian A, Tamayo P, Mootha VK, Mukherjee S, Ebert BL, Gillette MA, et al. Gene set enrichment analysis: a knowledge-based approach for interpreting genome-wide expression profiles. *Proc Natl Acad Sci U S A.* 2005;102:15545–50.

Submit your next manuscript to BioMed Central and take full advantage of:

- Convenient online submission
- Thorough peer review
- No space constraints or color figure charges
- Immediate publication on acceptance
- Inclusion in PubMed, CAS, Scopus and Google Scholar
- Research which is freely available for redistribution

Submit your manuscript at
www.biomedcentral.com/submit

